Title

Supercompliant and Soft (CH3NH3)3Bi2I9 Crystal with Ultralow Thermal Conductivity

Journal

Physical Review Letters, 123(15)

ISSN

0031-9007

Authors

Ma, Hao

Li, Chen

Ma, Yunwei

et al.

Publication Date

2019-10-11

DOI

10.1103/physrevlett.123.155901

Peer reviewed

Super Compliant and Soft $(CH_3NH_3)_3Bi_2I_9$ Crystals with Ultralow Thermal Conductivity

Hao Ma[1], Chen Li[1], Yunwei Ma[2], Heng Wang[3,4], Zachary W. Rouse[5], Zhuolei Zhang[3], Carla Slebodnick[6], Ahmet Alatas[7], Shefford P. Baker[5], Jeffrey J. Urban[3], and Zhiting Tian[1,2*]

[1]Sibley School of Mechanical and Aerospace Engineering, Cornell University, Ithaca, NY 14853, USA
[2]Department of Mechanical Engineering, Virginia Tech, Blacksburg, VA 24061, USA
[3]Molecular Foundry, Lawrence Berkeley National Laboratories, Berkeley, CA 94720, USA
[4]Department of Mechanical, Materials, and Aerospace Engineering, Illinois Institute of Technology, Chicago, IL 60616, USA
[5]Department of Materials Science and Engineering, Cornell University, Ithaca, NY 14853
[6]Department of Chemistry, Virginia Tech, Blacksburg, VA 24061, USA
[7]Advanced Photon Source, Argonne National Laboratory, Argonne, Illinois 64039, USA

Abstract

In this letter, we show the phonon dispersion of $(CH_3NH_3)_3Bi_2I_9$ single crystals at 300K as deduced from high energy resolution inelastic x-ray scattering measurements. The frequencies of acoustic phonons are among the lowest of all the reported crystals. Nanoindentation measurements verified that these crystals are very compliant and considerably soft. The frequency overlap between acoustic and optical phonons results in strong acoustic-optical scattering. All these features lead to an ultralow thermal conductivity. The fundamental knowledge obtained from this study will accelerate the design of novel hybrid materials for energy applications.

* Corresponding author. Email: zhiting@cornell.edu

Introduction

Fundamental understanding of phonon dynamics is essential to facilitating the optimization of thermal performance for hybrid perovskite devices. Organic-inorganic hybrid perovskite materials, such as methylammonium lead iodide ($CH_3NH_3PbI_3$), have attracted growing attention as absorber layers in photovoltaic materials since their first application in dye-sensitized solar cells in 2009[1]. Beside its utilization in solar cells, the potential applications of hybrid perovskite materials in thermoelectric applications[2-4] have also been reported. On one hand, high thermal conductivity is favorable for efficient heat dissipation to avoid adverse thermal degradation for hybrid perovskites in optoelectronic devices [5]. On the other hand, low thermal conductivity is beneficial for the hot-phonon bottleneck effect[6] to help achieve long-lived hot carrier photovoltaic device, and also desired for thermoelectrics[3].

Despite widespread interest in hybrid perovskites, the lead contained in $CH_3NH_3PbI_3$ can cause persistent environmental pollution. $CH_3NH_3PbI_3$ is also limited by its instability. Perovskite degradation readil occurs under extrinsic factors such as light[7], temperature[8], humidity[9] and oxygen[10], which makes it difficult to maintain efficient charge extraction with carrier-selective contacts. Less toxic counterparts have been proposed to replace Pb, such as $CH_3NH_3SnI_3$[11], but its potential application is also limited by its high instability[12]. Hybrid perovskite analogues, such as methylammonium bismuth iodide $(CH_3NH_3)_3Bi_2I_9$, have emerged as a candidate photovoltaic material[13,14] due to its low toxicity[15] and high stability[16]. While most previous studies reported very low power conversion efficiency (0.01-0.4%) [16-18], the efficiency of $(CH_3NH_3)_3Bi_2I_9$ has been pushed up to 1.64% by fabricating high-quality samples.[19] Moreover, a high efficiency (18.97%) and stable solar cell based on a $(CH_3NH_3)_3Bi_2I_9/CH_3NH_3PbI_3$ heterojunction has been achieved[20]. Increasing research on $(CH_3NH_3)_3Bi_2I_9$ has been done on electronic property simulations[21] and UV-vis absorption spectra[22]. However, its thermal transport properties are neither studied experimentally nor theoretically. Lack of phonon transport properties of hybrid perovskite analogue materials hinders the optimal selection and design of stable, non-toxic hybrid perovskite material for photovoltaic and thermoelectric applications.

In this letter, we present the phonon dispersion for $(CH_3NH_3)_3Bi_2I_9$ single crystals at room temperature using high energy resolution inelastic x-ray scattering (IXS) measurement. The acoustic modes of $(CH_3NH_3)_3Bi_2I_9$ are only up to 0.7 THz, which is among the lowest of all the reported crystals. Nanoindentation measurements confirmed that $CH_3NH_3)_3Bi_2I_9$ single crystals are very compliant with an averaged indentation modulus (E_{ind}) of 12.4 ± 0.8 GPa and considerably soft with a hardness of 471.2 ± 63.4 MPa. We observed no frequency gap between acoustic and optical branches in the

phonon dispersion, which could lead to strong acoustic-optical phonon scattering. Ultralow group velocities due to low-frequency acoustic phonons and small phonon lifetimes originating from strong acoustic-optical phonon coupling were expected to give ultralow thermal conductivity, which was confirmed by measured thermal conductivity of 0.23 ± 0.02 W/(mK) for $(CH_3NH_3)_3Bi_2I_9$ polycrystals at 300 K. The knowledge gained in our work provides a deeper understanding of thermal transport properties of hybrid perovskite analogue materials and can facilitate the design of novel hybrid materials with higher energy conversion efficiency and reliability.

Results and Discussion

We measured the phonon dispersion of $(CH_3NH_3)_3Bi_2I_9$ single crystals along high symmetry lines at 300 K using high energy resolution IXS as shown in FIG. 1. The detailed information on the crystal growth and characterization and IXS measurement could be found in the supporting information (SI). The phonon dispersion of the $(CH_3NH_3)_3Bi_2I_9$ single crystal using first-principles calculations is also shown in FIG. S2 in SI.

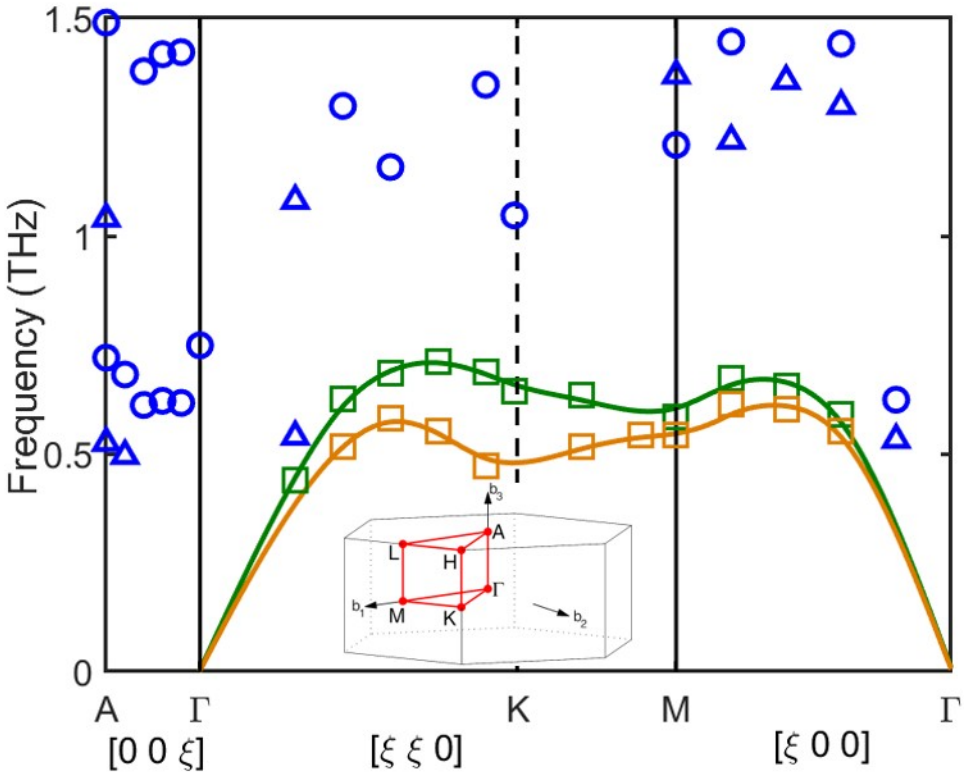

FIG. 1. Phonon dispersion of $(CH_3NH_3)_3Bi_2I_9$ single crystals measured by IXS at 300 K. The high symmetry points are chosen based on first Brillouin zone of hexagonal unit cell: Γ (0 0 0), A (0 0 0.5), K (0.33 0.33 0), M (0.5 0 0) in

unit of $(b_1, b_2, b_3¿$, where $b_1=\left(\frac{2\pi}{a}, \frac{2\pi}{\sqrt{3}a}, 0\right), b_2=\left(0, \frac{4\pi}{\sqrt{3}a}, 0\right), b_3=\left(0, 0, \frac{2\pi}{c}\right)$ in Cartesian coordinate system. The inset is the first Brillouin zone of $(CH_3NH_3)_3Bi_2I_9$ single crystal. Green squares, yellow squares, blue circles and blue triangles denote LA modes, TA modes, longitudinal optical (LO) modes and transverse optical (TO) modes, respectively.

Unique features are uncovered from phonon dispersion of $(CH_3NH_3)_3Bi_2I_9$. **I.** The most striking result is that the acoustic modes have low frequencies only up to around 0.7THz. To the best of our knowledge, this is the smallest frequency range for acoustic modes among all the reported crystalline materials. A comparison of acoustic phonon frequency ranges along high symmetry lines among different types of crystals is shown in FIG. 2a. Clearly, the frequencies of hybrid organic-inorganic crystals are the lowest, even lower than those of van der Waals (vdW) crystals[23-26]. This can be attributed to the weak electrostatic interactions between organic cations and inorganic units[27,28], which leads to large translational degrees of freedom for inorganic unit vibrations as the acoustic modes of hybrid organic-inorganic compounds are comprised of motions by the inorganic component. Notably, compared with the most popular hybrid perovskite $CH_3NH_3PbI_3$[29-32], $(CH_3NH_3)_3Bi_2I_9$ has even smaller acoustic frequencies, which can be attributed to the discontinuity of $Bi_2I_9^{3-}$ units[28]. The $Bi_2I_9^{3-}$ unit are isolated dimers of face-sharing octahedra that are separated by $CH_3NH_3^+$ in all three directions ([001], [100] and [110]), while in $CH_3NH_3PbI_3$, the inorganic component of corner sharing PbI_6 octahedra forms a three-dimensional framework, with $CH_3NH_3^+$ in the framework cages. Please refer to their crystal structures in FIG. S3 for more details. Therefore, interactions between the inorganic units are weaker in $(CH_3NH_3)_3Bi_2I_9$, leading to the overall lower frequency in phonon modes. **II.** The ultralow frequencies of acoustic phonons give exceptionally low average phonon group velocities – 1187 m/s in [100] direction, and 400 m/s in [110] direction that is even comparable to the speed of sound in air (Table SIII in SI)**.** Compared to tetragonal $CH_3NH_3PbI_3$ single crystals (Table SIV in SI), the overall phonon group velocities of $(CH_3NH_3)_3Bi_2I_9$ single crystals are even smaller. **III.** Both calculated and experimental phonon dispersion curves show a considerable frequency overlap between acoustic and optical branches. Specifically, both acoustic and optical phonon modes show up between 0.4 THz and 0.7 THz in the experimental dispersion. This overlap between acoustic and optical branches could result in strong coupling between them and significantly reduce the phonon lifetimes, as demonstrated in other materials[33,34]. This was further validated by that measured phonon lifetimes of acoustic phonon modes are mainly in a range of 1-30 ps in FIG. S4 in SI. We attribute the overlap between acoustic and optical modes to the coupling of $CH_3NH_3^+$

modes to stretching of the Bi-I bonds and breathing of the $Bi_2I_9^{3-}$ units, which is similar to $CH_3NH_3PbI_3$[35]. Based on all the features above, we anticipate $(CH_3NH_3)_3Bi_2I_9$ to have an ultralow thermal conductivity.

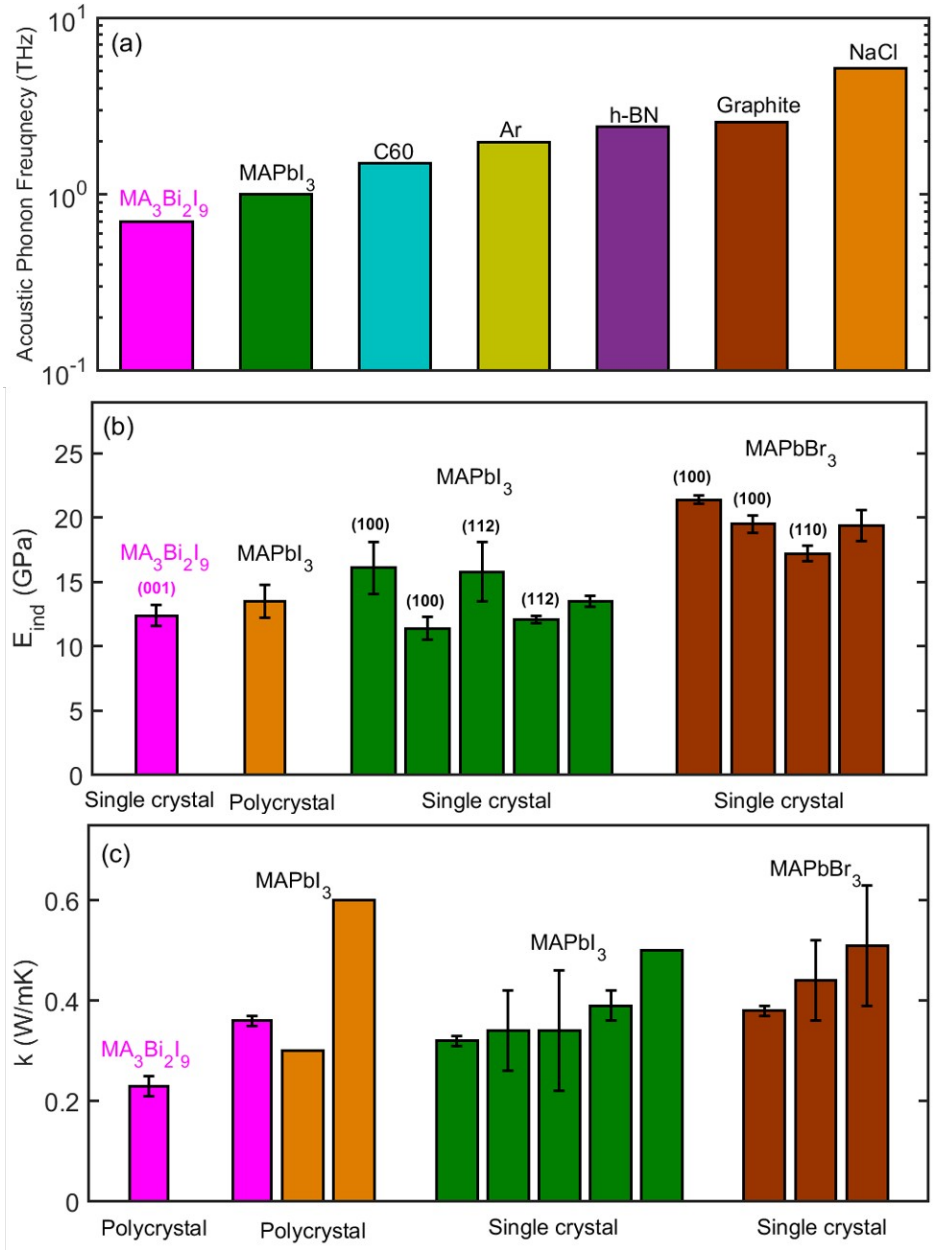

FIG. 2. (a) Comparison of acoustic phonon frequencies of different materials measured experimentally: $MA_3Bi_2I_9$ single crystals, tetragonal $MAPbI_3$ single crystals[31] (MA denotes $CH_3NH_3^+$), C60 (FCC)[23], argon (Ar) (FCC)[24], h-BN[25] and graphite[26] (cross-plane acoustic modes only), NaCl[36]. $MA_3Bi_2I_9$ and $MAPbI_3$ are hybrid organic-inorganic single crystals; C60, argon, h-BN and graphite are vdW crystals; NaCl is the ionic crystal. (b) Comparison of indentation modulus of different materials measured experimentally:

$MA_3Bi_2I_9$ single crystals, $MAPbI_3$ polycrystals[37], tetragonal $MAPbI_3$ single crystals[38-40], $MAPbBr_3$ single crystals[38-40]. Round brackets denote the orientation of the indented crystals. (c) Comparison of thermal conductivity of different materials measured experimentally at 300 K: $MA_3Bi_2I_9$ polycrystals, $MAPbI_3$ polycrystals[41,42], $MAPbI_3$ single crystals[40,41,43-45], $MAPbBr_3$ single crystals[43,44] [40]. Pink denotes the experimental results of this work.

The small phonon group velocities indicate low elastic modulus based on $v_s=\sqrt{\frac{E}{\rho}}$, where v_s, E and ρ are speed of sound, elastic modulus and the density, respectively[46]. To confirm the low elastic modulus, we performed nanoindentation measurements to obtain the indentation modulus of $(CH_3NH_3)_3Bi_2I_9$ single crystals and more details could be found in the SI. $(CH_3NH_3)_3Bi_2I_9$ single crystals are very compliant with an averaged indentation modulus (E_{ind}) of 12.4 ± 0.8 GPa. We did not convert it to Young's modulus for the following reasons: Extracting Young's modulus (E_{smp}) requires the assumption that the material is isotropic with a single invariant value for Poisson ratio (ν_{smp}). ν_{smp} of $(CH_3NH_3)_3Bi_2I_9$ single crystals remains unknown. Moreover, E_{ind} is the basic quantity obtained from a nanoindentation experiment, which can be directly compared. By contrast, Young's modulus is only meaningful for a uniaxial test. In order to compare the E_{ind} values of $(CH_3NH_3)_3Bi_2I_9$ to other similar crystals, for studies that reported E_{smp} rather than E_{ind}, the values of E_{ind} were calculated using ν_{smp} specified in their work. Moduli derived from indentation tests were plotted in FIG. 2b and tabulated in Table SV. We found that indentation modulus of $(CH_3NH_3)_3Bi_2I_9$ single crystals is slightly smaller than that of $CH_3NH_3PbI_3$ crystals but much lower than that of $CH_3NH_3PbBr_3$ single crystals, indicating their super compliant feature. The hardness of $(CH_3NH_3)_3Bi_2I_9$ single crystals was found to be 471.2 ± 63.4 MPa, which is lower than the reported hardness of $CH_3NH_3PbI_3$ single crystals: 570 MPa for (100) face and 550 MPa for (112) face [38]. It demonstrates that $(CH_3NH_3)_3Bi_2I_9$ single crystals are softer than $CH_3NH_3PbI_3$ single crystals. In brief, $(CH_3NH_3)_3Bi_2I_9$ single crystals are super compliant and soft.

To demonstrate the ultralow thermal conductivity, we measured thermal conductivity of both $(CH_3NH_3)_3Bi_2I_9$ and $CH_3NH_3PbI_3$ polycrystals using the laser flash method to have a direct comparison and details could be found in SI[47]. We found that thermal conductivity of $CH_3NH_3PbI_3$ polycrystals is 0.36±0.01 W/(mK) at 300 K, which falls into the range of previous reported values (0.3 W/(mK)[41], 0.6 W/(mK)[42]). Thermal conductivity of $(CH_3NH_3)_3Bi_2I_9$ polycrystals is 0.23±0.02 W/(mK) at 300 K, which is

significantly lower than that of $CH_3NH_3PbI_3$ polycrystals under the same measurement conditions and lower than the reported thermal conductivity values of all the hybrid perovskites as shown in FIG. 2c and Table SVI in SI. Note that the grain size of $(CH_3NH_3)_3Bi_2I_9$ and $CH_3NH_3PbI_3$ polycrystals in this study is larger than 2 μm so that grain boundary has little impact on thermal conductivity.[47] It is further supported by the comparable thermal conductivity of our measured $CH_3NH_3PbI_3$ polycrystals and previous reported $CH_3NH_3PbI_3$ sing crystals in FIG. 2c. Nevertheless, despite the well-defined crystal structure, the thermal conductivity of $(CH_3NH_3)_3Bi_2I_9$ is ultralow and comparable to thermal conductivity of most amorphous polymers.

Conclusions

In summary, we measured the phonon dispersion of hybrid perovskite analogue $(CH_3NH_3)_3Bi_2I_9$ to provide the first dataset of intrinsic phonon properties of $(CH_3NH_3)_3Bi_2I_9$. Remarkably, we observed its acoustic frequency range is the smallest among reported crystalline materials, to the best of our knowledge. The ultralow-frequency acoustic phonon modes may result from the weak electrostatic force between organic and inorganic units and the discontinuous inorganic units in [001], [100] and [110] directions. Based on the low frequencies of phonon modes, the ultralow group velocities were expected and then supported by nanoindentation measurements. It reveals that $CH_3NH_3)_3Bi_2I_9$ single crystals are super compliant and considerably soft. The phonon dispersion also shows a considerable acoustic-optical overlap, which could lead to strong acoustic-optical coupling and thus small phonon lifetimes. The thermal conductivity of $(CH_3NH_3)_3Bi_2I_9$ polycrystals was expected to be ultralow due to these unique features and was validated by the laser flash measurements. This work provided valuable benchmark data of thermal transport properties of $(CH_3NH_3)_3Bi_2I_9$ for future studies and identified unique phonon properties for the design of ultralow thermal conductivity materials.

Acknowledgements

This work was funded by Z.T.'s NSF CAREER Award (CBET-1839384). This work was supported by the Molecular Foundry at Lawrence Berkeley National Laboratory, a user facility supported by the Office of Science, Office of Basic Energy Sciences, of the U.S. Department of Energy (DOE) under Contract No. DE-AC02-05CH11231. This research used resources of the Advanced Photon Source, a U.S. Department of Energy (DOE) Office of Science User Facility operated for the DOE Office of Science by Argonne National Laboratory under Contract No. DE-AC02-06CH11357.

References

[1] A. Kojima, K. Teshima, Y. Shirai, and T. Miyasaka, J. Am. Chem. Soc. **131**, 6050 (2009).

[2] C. Lee, J. Hong, A. Stroppa, M.-H. Whangbo, and J. H. Shim, Rsc Advances **5**, 78701 (2015).
[3] Y. He and G. Galli, Chemistry of Materials **26**, 5394 (2014).
[4] X. Mettan *et al.*, The Journal of Physical Chemistry C **119**, 11506 (2015).
[5] A. Pisoni, J. Jacimovic, O. S. Barisic, M. Spina, R. Gaál, L. Forró, and E. Horváth, The journal of physical chemistry letters **5**, 2488 (2014).
[6] J. Yang *et al.*, Nature communications **8**, 14120 (2017).
[7] Y. Li, X. Xu, C. Wang, B. Ecker, J. Yang, J. Huang, and Y. Gao, The Journal of Physical Chemistry C **121**, 3904 (2017).
[8] R. K. Misra, S. Aharon, B. Li, D. Mogilyansky, I. Visoly-Fisher, L. Etgar, and E. A. Katz, The Journal of Physical Chemistry Letters **6**, 326 (2015).
[9] J. Yang, B. D. Siempelkamp, D. Liu, and T. L. Kelly, ACS nano **9**, 1955 (2015).
[10] N. Aristidou, I. Sanchez-Molina, T. Chotchuangchutchaval, M. Brown, L. Martinez, T. Rath, and S. A. Haque, **54**, 8208 (2015).
[11] N. K. Noel *et al.*, Energy & Environmental Science **7**, 3061 (2014).
[12] T. Fujihara, S. Terakawa, T. Matsushima, C. Qin, M. Yahiro, and C. Adachi, Journal of Materials Chemistry C **5**, 1121 (2017).
[13] B. W. Park, B. Philippe, X. Zhang, H. Rensmo, G. Boschloo, and E. M. Johansson, Advanced Materials **27**, 6806 (2015).
[14] M. Lyu *et al.*, Nano Research **9**, 692 (2016).
[15] T. Okano and Y. Suzuki, Materials Letters **191**, 77 (2017).
[16] C. Ran, Z. Wu, J. Xi, F. Yuan, H. Dong, T. Lei, X. He, and X. Hou, The journal of physical chemistry letters **8**, 394 (2017).
[17] B.-W. Park, B. Philippe, X. Zhang, H. Rensmo, G. Boschloo, and E. M. J. Johansson, **27**, 6806 (2015).
[18] S. Öz *et al.*, Solar Energy Materials and Solar Cells **158**, 195 (2016).
[19] Z. Zhang, X. Li, X. Xia, Z. Wang, Z. Huang, B. Lei, and Y. Gao, The Journal of Physical Chemistry Letters **8**, 4300 (2017).
[20] Y. Hu, T. Qiu, F. Bai, W. Ruan, and S. Zhang, Advance Energy Materials **8**, 1703620 (2018).
[21] A. Koliogiorgos, S. Baskoutas, and I. Galanakis, arXiv preprint arXiv:1711.04846 (2017).
[22] X. Chen *et al.*, Journal of Materials Chemistry A **5**, 24728 (2017).
[23] L. Pintschovius, B. Renker, F. Gompf, R. Heid, S. L. Chaplot, M. Haluska, and H. Kuzmany, Physical Review Letters **69**, 2662 (1992).
[24] Y. Fujii, N. A. Lurie, R. Pynn, and G. Shirane, Physical Review B **10**, 3647 (1974).
[25] J. Serrano, A. Bosak, R. Arenal, M. Krisch, K. Watanabe, T. Taniguchi, H. Kanda, A. Rubio, and L. Wirtz, Physical Review Letters **98**, 095503 (2007).
[26] R. Nicklow, N. Wakabayashi, and H. G. Smith, Physical Review B **5**, 4951 (1972).
[27] J. M. Frost, K. T. Butler, F. Brivio, C. H. Hendon, M. van Schilfgaarde, and A. Walsh, Nano Letters **14**, 2584 (2014).
[28] A. Walsh, The Journal of Physical Chemistry C **119**, 5755 (2015).

[29] M. Wang and S. Lin, Advanced Functional Materials **26**, 5297 (2016).
[30] S.-Y. Yue, X. Zhang, G. Qin, J. Yang, and M. Hu, Physical Review B **94**, 115427 (2016).
[31] Hao Ma, Yunwei Ma, Heng Wang, Carla Slebodnick, Ahmet Alatas, Jeffery J. Urban, Zhiting Tian.
[32] A. N. Beecher *et al.*, ACS Energy Letters **1**, 880 (2016).
[33] Z. Tian, J. Garg, K. Esfarjani, T. Shiga, J. Shiomi, and G. Chen, Physical Review B **85**, 184303 (2012).
[34] S. Lee, K. Esfarjani, T. Luo, J. Zhou, Z. Tian, and G. Chen, Nature communications **5**, 3525 (2014).
[35] F. Brivio *et al.*, Physical Review B **92**, 144308 (2015).
[36] G. Raunio, L. Almqvist, and R. J. P. R. Stedman, **178**, 1496 (1969).
[37] M. Park, H. J. Kim, I. Jeong, J. Lee, H. Lee, H. J. Son, D.-E. Kim, and M. J. Ko, **5**, 1501406 (2015).
[38] Y. Rakita, S. R. Cohen, N. K. Kedem, G. Hodes, and D. Cahen, MRS Communications **5**, 623 (2015).
[39] S. Sun, Y. Fang, G. Kieslich, T. J. White, and A. K. Cheetham, Journal of Materials Chemistry A **3**, 18450 (2015).
[40] G. A. Elbaz, W.-L. Ong, E. A. Doud, P. Kim, D. W. Paley, X. Roy, and J. A. Malen, Nano Letters **17**, 5734 (2017).
[41] A. Pisoni, J. Jaćimović, O. S. Barišić, M. Spina, R. Gaál, L. Forró, and E. Horváth, The Journal of Physical Chemistry Letters **5**, 2488 (2014).
[42] A. Kovalsky, L. Wang, G. T. Marek, C. Burda, and J. S. Dyck, The Journal of Physical Chemistry C **121**, 3228 (2017).
[43] C. Ge, M. Hu, P. Wu, Q. Tan, Z. Chen, Y. Wang, J. Shi, and J. Feng, The Journal of Physical Chemistry C **122**, 15973 (2018).
[44] R. Heiderhoff, T. Haeger, N. Pourdavoud, T. Hu, M. Al-Khafaji, A. Mayer, Y. Chen, H.-C. Scheer, and T. Riedl, The Journal of Physical Chemistry C **121**, 28306 (2017).
[45] T. Ye, X. Wang, X. Li, A. Q. Yan, S. Ramakrishna, and J. Xu, Journal of Materials Chemistry C **5**, 1255 (2017).
[46] W. Kim, Journal of Materials Chemistry C **3**, 10336 (2015).
[47] X. Long, Z. Pan, Z. Zhang, J. J. Urban, and H. Wang, **115**, 072104 (2019).